Journal of Biomolecular NMR, **14:** 181–184, 1999.
KLUWER/ESCOM

Measurement of $^{3h}J_{NC'}$ connectivities across hydrogen bonds in a 30 kDa protein

Yun-Xing Wang[a], Jaison Jacob[a], Florence Cordier[b], Paul Wingfield[c], Stephen J. Stahl[c], Sylvia Lee-Huang[d], Dennis Torchia[a], Stephan Grzesiek[b,e] & Ad Bax[f]

[a]*Molecular Structural Biology Unit, National Institute of Dental Research, National Institutes of Health, Bethesda, MD 20892-0520, U.S.A.;* [b]*Institute of Structural Biology, Forschungszentrum Jülich, D-52425 Jülich, Germany;* [c]*Protein Expression Laboratory, National Institute of Arthritis and Musculoskeletal and Skin Diseases, National Institutes of Health, Bethesda, MD 20892-0520, U.S.A.;* [d]*Department of Biochemistry, New York University School of Medicine, New York, NY 10016, U.S.A.;* [e]*Institute of Physical Biology, Heinrich-Heine Universität, D-40225 Düsseldorf, Germany;* [f]*Laboratory of Chemical Physics, National Institute of Diabetes and Digestive and Kidney Diseases, National Institutes of Health, Bethesda, MD 20892-0520, U.S.A.*

Received 6 April 1999; Accepted 22 April 1999

Key words: hydrogen bond, J coupling, MAP30, perdeuteration, relaxation rates, TROSY

Abstract

A method is described which permits detection of $^{3h}J_{NC'}$ scalar couplings across hydrogen bonds in larger, perdeuterated proteins. The experiment is demonstrated for the uniformly $^{2}H/^{13}C/^{15}N$-enriched 30 kDa ribosome inactivating protein MAP30. The $^{3h}J_{NC'}$ interactions are smaller than 1 Hz, but their detection in an HNCO experiment is made possible through the use of constructive interference between the ^{15}N chemical shift anisotropy and ^{1}H-^{15}N dipole-dipole relaxation mechanisms in a manner similar to that of recently proposed TROSY schemes. Sensitivity of the HNCO experiment depends strongly on the ^{15}N transverse relaxation rate of the downfield ^{15}N multiplet component and on the amide proton T_1. In perdeuterated MAP30 at 40 °C, the average TROSY T_2 was 169 ms at 750 MHz ^{1}H frequency, and a wide range of longitudinal relaxation rates was observed for the amide protons.

Hydrogen bonds are of fundamental importance in stabilizing biomolecular structure, and play key roles in nearly all enzymatic reactions. Recently, the presence of large J couplings (6–7 Hz) between the hydrogen bond (H-bond) donating and accepting ^{15}N nuclei in Watson–Crick basepairs in double-stranded RNA was reported by Dingley and Grzesiek (1998). This finding was confirmed by Pervushin et al. (1998a), and these authors additionally discovered the presence of a smaller (2–4 Hz) J coupling between the imino hydrogen itself and the H-bond accepting ^{15}N nucleus. The presence of J coupling confirms the presence of overlap between the electronic orbitals of the atoms involved, and equally importantly, such J coupling identifies unambiguously the pairs of atoms involved in a given H-bond. Very recently, analogous through-hydrogen-bond J couplings, $^{3h}J_{NC'}$, between the H-bond donating amide ^{15}N and the accepting carbonyl $^{13}C'$ nucleus have been observed in regular backbone-backbone and backbone-sidechain H-bonds in proteins (Cordier and Grzesiek, 1999; Cornilescu et al., 1999a,b). The magnitude of the $^{3h}J_{NC'}$ coupling decreases exponentially with increasing H-bond length (Cornilescu et al., 1999b), and typically is smaller than 1 Hz for regular, weak H-bonds in proteins. Observation of connectivity through the small $^{3h}J_{NC'}$ coupling is limited by the line width of the ^{15}N and $^{13}C'$ nuclei in proteins, and so far detection of $^{3h}J_{NC'}$ couplings has been restricted to small (<10 kDa) proteins. Here, we demonstrate that constructive relaxation interference between the ^{15}N chemical shift anisotropy and ^{1}H-^{15}N dipole-dipole relaxation mechanisms can be

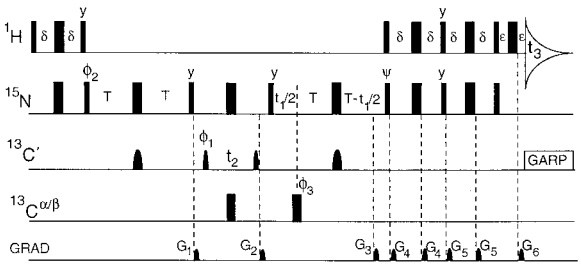

Figure 1. Pulse scheme of the water-flip-back 3D $^{3h}J_{NC'}$ HNCO experiment, used to detect through-hydrogen bond J connectivities in medium-size proteins. Narrow and wide pulses correspond to flip angles of 90° and 180°, respectively. All pulse phases are *x*, unless specified. $^{13}C'$ pulses have the shape of the center lobe of a $\sin x/x$ function, and durations of 150 μs. Shaped $^{13}C'$ pulses at the midpoint of the 2T periods are 180°; pulses bracketing the $^{13}C'$ t_2 evolution period are of lower power and correspond to 90°. Delay durations: $\delta = 2.65$ ms; $T = 66.6$ ms $\approx 1/^1J_{NC'}$. Phase cycling: $\psi = -x$; $\phi_1 = x, -x$; $\phi_2 = 2(x),2(-x)$; $\phi_3 = 4(x),4(-x)$. Receiver = x,2(−x),x. In order to obtain Rance–Kay style quadrature data in the t_1 dimension, the phase ψ is inverted in concert with inversion of gradient G_3, with data stored separately. Gradients are sine-bell shaped, with peak amplitudes of 30 G/cm, and durations $G_{1,2,3,4,5,6} = 0.7, 1.3, 2.705, 1, 1, 0.275$ ms, and directions y, −y, z, x, y, and z, respectively. For the reference spectrum, the $^{13}C'$ 180° pulses are applied 16.6 ms prior to the ^{15}N 180° pulses at the midpoints of the 2T periods (Cordier and Grzesiek, 1999), and a two-step phase cycle suffices. For including the Boltzmann ^{15}N magnetization, the 90° ^{1}H pulse at the end of the first INEPT transfer must be applied along the y axis (as shown) on Bruker spectrometers, but along −y on Varian-type instruments (Zhu et al., 1999).

used to observe such connectivities in a protein of 30 kDa.

The pulse scheme used for detection of $^{3h}J_{NC'}$ connectivity is shown in Figure 1. It is very similar to the schemes previously used for smaller proteins (Cordier and Grzesiek, 1999; Cornilescu et al., 1999a), but differs by the lack of ^{1}H composite pulse decoupling during the long ^{15}N-$^{13}C'$ de/rephasing intervals. Instead, the present scheme aims to observe only the magnetization transfer associated with the downfield ^{15}N-{^{1}H} doublet component. As a result of relaxation interference between the ^{15}N chemical shift anisotropy and dipole-dipole relaxation mechanisms, the transverse relaxation rate of the downfield ^{15}N doublet component is much smaller than that of the upfield components, whereas for the amide proton the opposite is the case (Goldman, 1984; Tjandra et al., 1996; Tjandra and Bax, 1997; Tessari et al., 1997). Pervushin et al. (1997, 1998a) developed an effective method for selectively observing this narrow component, and for optimizing magnetization transfer between the narrowest ^{15}N and $^1H^N$ components.

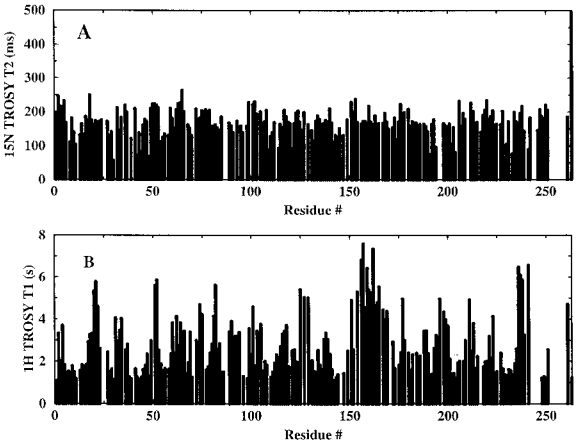

Figure 2. Relaxation times in 85%-perdeuterated, 98% $^{15}N/^{13}C$-labeled MAP30, at 750 MHz ^{1}H frequency, 40 °C. (A) ^{15}N T_2 relaxation times of the downfield ^{15}N doublet component. No attempt was made to decouple ^{13}C during the transverse relaxation delay, and the T_2 values include the effect of $^{13}C^\alpha$ and $^{13}C'$ spin flips during this delay. (B) Effective $^1H^N$ T_1 in the absence of ^{15}N decoupling or pulsing (see text).

This so-called TROSY method can yield resolution and sensitivity enhancement in heteronuclear triple resonance experiments of isotopically labeled proteins (Salzmann et al., 1999; Yang and Kay, 1999a,b).

The pulse scheme shown in Figure 1 is essentially an HNCO triple resonance experiment (Kay et al., 1990; Grzesiek and Bax, 1992), but uses very long ^{15}N-{$^{13}C'$} de/rephasing periods, 2T, that are tuned to $2/^1J_{NC'}$ (133 ms), such that magnetization transfer from a backbone ^{15}N to its preceding $^{13}C'$ is minimized. ^{15}N transverse magnetization at the beginning of the first 2T period consists of an antiphase $2N_yH_z$ term. Writing $2N_yH_z = [(1+ 2H_z)N_y - (1 - 2H_z)N_y]/2$ decomposes this into separate terms for the downfield, $^1/_2(1 - 2H_z)N_y$, doublet component and the fast relaxing upfield component, $^1/_2(1 + 2H_z)N_y$. This latter component can be safely ignored as it rapidly decays during the subsequent long ^{15}N de/rephasing delays, 2T. The slowly relaxing downfield component is larger than what is obtained from the INEPT transfer alone, as it also contains a component originating from the ^{15}N Boltzmann magnetization, present before the start of the pulse sequence (Pervushin et al., 1998b). This increases the amount of $(1 - 2H_z)N_y$ magnetization (see legend to Figure 1).

Dephasing caused by $^{3h}J_{NC'}$ during the first 2T period yields antiphase terms of the type $(1 - 2H_z)$ $\sin(2\pi\ ^{3h}J_{NC'}\ T)\ N_xC'_z$, just prior to the first 90°_y ^{15}N pulse. At the start of the t_2 $^{13}C'$ evolution pe-

riod this term is converted into $(1 - 2H_z)N_zC'_y$, which corresponds to transverse $^{13}C'$ magnetization of the H-bonded carbonyl group. At the end of the t_2 period, magnetization is transferred back to $(1 - 2H_z)N_xC'_z$. After the constant-time t_1 evolution period, of total duration 2T, the ^{15}N magnetization which has rephased with respect to $^{13}C'$ is proportional to $\sin^2(2\pi\ ^{3h}J_{NC'}\ T)\ N_y\ (1 - 2H_z)$. The subsequent gradient-enhanced magnetization transfer scheme converts $N_y(1 - 2H_z)$ into $H_x(1 - 2N_z)$, which corresponds to the upfield $^1H^N$-{^{15}N} component (Yang and Kay, 1999a,b). Phase encoding is accomplished with gradient G_3, and decoding with G_6. Note that the pulse scheme reaps the benefit of 'water-flip-back' (Grzesiek and Bax, 1993) as H_2O magnetization is actively restored to the $+z$ axis at the end of the pulse scheme. No selective water flip-back pulse is needed after the first $^1H \rightarrow {}^{15}N$ INEPT transfer, as the ^1H magnetization is in the transverse plane after the 90°_y ^1H pulse, and radiation damping effectively returns it to $+z$. The sum of all rotations in the gradient enhanced back transfer, preceding t_3, equals 720°, and therefore leaves water magnetization along $+z$ prior to detection.

The experiment is demonstrated for a 0.7 mM sample of the ribosome inactivating protein MAP30 (263 residues; 30 kDa) in 300 µl H_2O/D_2O, pH 5.5, 10 mM phosphate buffer. The protein was uniformly enriched in ^2H, ^{13}C, and ^{15}N. Experiments were carried out on a Bruker DMX750 spectrometer, equipped with a triple resonance 3-axis pulsed field gradient probehead. The 3D HNCO flip-back spectrum was recorded with the scheme of Figure 1, as a $99^* \times 32^* \times 768^*$ data matrix with acquisition times of 65 ms (t_1), 14 ms (t_2) and 79 ms (t_3). The data were acquired with 8 scans per FID, i.e., 32 scans per hypercomplex t_1/t_2 increment, with an interscan delay of 2.6 s, and a total measuring time of 3.8 days. The t_1 time domain data were doubled by mirror image linear prediction in the t_1 dimension (Zhu and Bax, 1990) and similarly, the t_2 domain was extended to 64^* data points by backward/forward linear prediction (Zhu and Bax, 1992). The protocol described in Figure 5 of Delaglio et al. (1995) was used to obtain optimal linear prediction in two dimensions.

In order to evaluate feasibility of the through-H-bond HNCO experiment, we also carried out a T_2 measurement of the downfield ^{15}N doublet component by inserting a (delay-180°-delay) prior to ^{15}N evolution, and measuring the intensity in the TROSY spectrum as a function of this spin echo delay. Results are summarized in Figure 2A. The average T_2 over 219 non-overlapping backbone amides was found to be 169 ± 45 ms. This standard deviation is relatively large, and for 50 amides T_2 values exceed 200 ms. At the high field strength used, the TROSY T_2 values are exquisitely sensitive to conformational exchange broadening, and many of the residues with short (<120 ms) T_2 are localized in loop regions. Variations in the magnitude and orientation of the ^{15}N CSA tensor are known to be quite significant (Tjandra et al., 1996; Fushman et al., 1998), and this also constitutes a significant source of variations in the TROSY T_2 values. Another potentially significant source stems from the non-uniformity in ^1H spin density, which causes different amide proton spins to undergo spin-flips at different rates.

The MAP30 protein was expressed in *E. coli*, using a medium containing 98% D_2O but protonated ^{13}C glucose. As a result, deuteration of non-exchanging sites in MAP30 is only about 85% complete. In order to evaluate the optimum rate at which to repeat the 3D HNCO experiment, it is important to have a good estimate for the H^N longitudinal relaxation times. These were calculated from the relative intensities observed in water-flip-back TROSY spectra, recorded at 2.5 and 5 s delay between scans (including the data acquisition period). A two-step phase cycle of the $90_{\pm y}$ ^1H pulse at the end of the first INEPT ensures that the ^{15}N Boltzmann component (Pervushin et al., 1998b) does not contribute to the observed signal. A wide range of $^1H^N$ T_1 values is seen (Figure 2B), and many amides in the core of the protein show particularly long T_1 values. Amide ^1H T_1 relaxation is non-exponential, and values shown correspond to the average rate of recovery during the 2.5 to 5 s interval after the ^1H nuclear spin magnetization is saturated. We expect it will be possible to increase the $^1H^N$ recovery rates by ensuring that not only the water magnetization but also the magnetization of ^{13}C-attached protons is returned to the *z* axis at the end of the pulse sequence, but no such modification was incorporated here. Although from an S/N perspective, a ∼5 s delay between scans would have been optimal for MAP30, the minimum time needed to record the HNCO reference spectrum at the required 3D resolution would have been unacceptably long, and a compromise delay duration of 2.6 s was used instead.

Figure 3 shows $^{13}C'$ strips of residues in the 9th and 10th β-strand of MAP30, taken from the 3D through-H-bond HNCO spectrum. A reference spec-

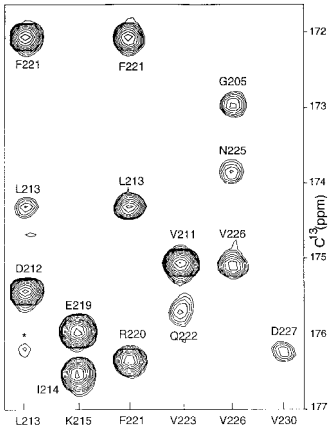

Figure 3. Strip plot of the 3D $^{3h}J_{NC'}$ HNCO spectrum of MAP30, showing through-hydrogen-bond J correlations involving amides of the 9th and 10th β-strands. The strips are labeled by the residue of the amide resonance detected during t_3, and cross peaks to carbonyls are marked by their corresponding residues. Correlations resulting from small $^{2}J_{NC'}$ couplings are observed for L213, F221 and V226.

trum with 2 scans per FID was also recorded (data not shown), and showed a substantial range in peak intensities which largely reflect the variations in the TROSY T_2 value and the effective $^{1}H^{N}$ T_1, but are also affected by incomplete back exchange after the protein expressed in D_2O was transferred to H_2O. In fact, about 40 of the most strongly H-bonded amide protons have greatly diminished or undetectable intensity in the TROSY and HSQC spectra as a result of this incomplete back exchange. Unfortunately, these are exactly the amides which are expected to yield the strongest $^{3h}J_{NC'}$ connectivities, and the total number of observed $^{3h}J_{NC'}$ connectivities was only 65. Their magnitude was calculated from the relative intensity in the reference and through-H-bond HNCO spectra (Cordier and Grzesiek, 1999; Cornilescu et al., 1999), and observed values range from 0.25 Hz for K84 to 0.82 Hz for L125.

We have shown that use of TROSY ^{15}N line narrowing makes it possible to detect the very small $^{3h}J_{NC'}$ (< 1 Hz) connectivities in a relatively large protein of 30 kDa. These connectivities provide the all-important link between the donor and acceptor atoms and are extremely useful in structure calculations. MAP30 has favorable NMR characteristics for a protein this large: it is highly stable and permits measurements at high temperature (40 °C) for extended periods of time. However, at 263 residues it is among the largest single chain proteins for which a structure has been determined by NMR (Y.-X. Wang, unpublished results). This suggests that $^{3h}J_{NC'}$ connectivities can be measured in the majority of proteins whose structure is being studied by NMR, provided deuteration is used. In the absence of perdeuteration, the TROSY increase of the ^{15}N T_2 is considerably smaller, making it very difficult to detect the $^{3h}J_{NC'}$ connectivities, even in medium-size proteins.

Acknowledgements

We thank G.M. Clore and F. Delaglio for useful discussions. This work was supported by a fellowship from the A. v. Humboldt foundation (F.C.), DFG grant GR1683/1-1 (S.G.), and the AIDS Targeted Anti-Viral Program of the Office of the Director of the National Institutes of Health (D.A.T. and A.B.).

References

Cordier, F. and Grzesiek, S. (1999) *J. Am. Chem. Soc.*, **121**, 1601–1602.

Cornilescu, G., Hu, J.-S. and Bax, A. (1999a) *J. Am. Chem. Soc.*, **121**, 2949–2950.

Cornilescu, G., Ramirez, B.E., Frank, M.K., Clore, G.M., Gronenborn, A.M. and Bax, A. (1999b) *J. Am. Chem. Soc.*, in press.

Delaglio, F., Grzesiek, S., Vuister, G.W., Zhu, G., Pfeifer, J. and Bax, A. (1995) *J. Biomol. NMR*, **6**, 277–293.

Dingley, A.J. and Grzesiek, S. (1998) *J. Am. Chem. Soc.*, **120**, 8293–8297.

Fushman, D., Tjandra, N. and Cowburn, D. (1998) *J. Am. Chem. Soc.*, **120**, 10947–10952.

Goldman, M. (1984) *J. Magn. Reson.*, **60**, 437–452.

Grzesiek, S. and Bax, A. (1993) *J. Am. Chem. Soc.*, **115**, 12593–12594.

Pervushin, K., Riek, R., Wider, G. and Wüthrich, K. (1997) *Proc. Natl. Acad. Sci. USA*, **94**, 12366–12371.

Pervushin, K., Ono, A., Fernandez, C., Szyperski, T., Kainosho, M. and Wüthrich, K. (1998a) *Proc. Natl. Acad. Sci. USA*, **95**, 14147–14151.

Pervushin, K., Wider, G. and Wüthrich, K. (1998b) *J. Biomol. NMR*, **12**, 345–348.

Salzmann, M., Wider, G., Pervushin, K., Senn, H. and Wüthrich, K. (1999) *J. Am. Chem. Soc.*, **121**, 844–848.

Tjandra, N., Szabo, A. and Bax, A. (1996) *J. Am. Chem. Soc.*, **118**, 6986–6991.

Tjandra, N. and Bax, A. (1997) *J. Am. Chem. Soc.*, **119**, 8076–8082.

Tessari, M., Vis, H., Boelens, R., Kaptein, R. and Vuister, G.W. (1997) *J. Am. Chem. Soc.*, **119**, 8985–8990.

Yang, D. and Kay, L.E. (1999a) *J. Biomol. NMR*, **13**, 3–10.

Yang, D. and Kay, L.E. (1999b) *J. Am. Chem. Soc.*, **121**, 2571–2575.

Zhu, G. and Bax, A. (1990) *J. Magn. Reson.*, **90**, 405–410.

Zhu, G. and Bax, A. (1992) *J. Magn. Reson.*, **100**, 202–207.

Zhu, G., Kong, X.M. and Sze, K.H. (1999) *J. Biomol. NMR*, **13**, 77–81.